Ultra-Miniature Dual-Band Antenna Based on Subwavelength Resonators on $LiNbO_3$ Substrate

A.E. Serebryannikov[1], M. Gokkavas[2], F.T. Gundogdu[2], G.A.E. Vandenbosch[1], A. Vasylchenko[3], E. Ozbay[2]
[1] Department of Electrical Engineering, Katholieke Universiteit Leuven, Leuven, Belgium, aserebry@esat.kuleuven.be
[2] NANOTAM - Nanotechnology Research Center, Bilkent University, Ankara, Turkey, gokkavas@bilkent.edu.tr
[3] Sofitto NV, Leuven, Belgium

***Abstract*— The common effect of subwavelength resonators and a high-permittivity lithium niobate substrate is used for deep-subwavelength miniaturization of a dual-band S/C-band monopole antenna. The resulting size is just about 1/18th of a wavelength for the lower band.**

***Index Terms*—ultra-miniature antenna, subwavelength resonators, lithium niobate.**

I. Introduction

The interest in open subwavelength resonators and thereof derived metamaterials has been growing since the early 2000's [1-3]. Being initially suggested for obtaining a negative refraction, subwavelength resonators enable a dramatic miniaturization of microwave devices. Progress in this direction provided new solutions for small antennas and new insight in operation and design of small antennas of the existing types [4-12]. They include the ones based on metamaterials and metasurfaces, as well as those based on their unit cells that typically comprise one or two subwavelength resonators.

At the same time, increasing the substrate permittivity is a natural and widely used way of miniaturization of microwave and millimeter-wave devices [13]. The higher the permittivity, the longer the in-material wavelength is and the more compact the resulting device can be. For antennas using subwavelength resonators (SRRs or similar), a trade-off between Q-factor and bandwidth, on the one hand, and the extent of miniaturization, on the other hand, is required when choosing material and size of substrate. Moreover, it can be challenging to keep sizes of a miniaturized antenna smaller than $\lambda_0/4$ for all bands when multiband operation is required, so that different bands should correspond to different communication standards. From the open resonator perspective, the problem is not trivial because possible shifts of resonance frequencies due to variations of substrate permittivity cannot be quantified a priori, i.e., without extensive simulations [14].

High demand in (ultra-)miniature antennas for IoT [15,16], medical [17], and mobile phone [18,19] applications stimulated the recent progress in antenna miniaturization. In this concern, the challenges towards decreasing the maximal size below $\lambda_0/20$ should be mentioned. In addition to the antennas on commercial high-ε ceramic substrates, efforts have been made to design such small antennas by using more conventional materials. In particular, such ultra-miniature antennas for IoT applications have been proposed, based on either an IFA [15] or a split-ring-like structure [16].

In this paper, we present the first results of a theoretical and experimental study of ultra-miniature, dual-band, S/C-band antennas fed by a coaxial cable, which are enabled by the common effect of subwavelength resonances and a high-permittivity substrate. The reasons of low cost and wide use in electrical engineering encourage the choice of $LiNbO_3$ as a substrate. It has been commonly used in electrooptics in modulators and converters, as well as in patch and bow-tie antennas being a part of these electrooptical devices [20-24]. To the best of our knowledge, $LiNbO_3$ has not yet been used in small antennas beyond electrooptics, i.e., just for the purpose of miniaturization. The presented results demonstrate that a proper combination of resonator and substrate properties in a low-profile antenna yields a desirably high extent of miniaturization, so that both used resonances remain deeply subwavelength.

II. Design and Fabrication

The proposed antenna represents two embedded split square-shaped resonators on a thin square $LiNbO_3$ substrate, which are placed nearby the extended inner conductor of the feeding coaxial cable, as shown in Fig. 1. Simulations are performed with CST Microwave Studio. Spectral locations of the resonances are retrieved from the S11 data. It has been shown that the resonances of the original, substrate-free (hypothetic) antenna fed by the coaxial cable are gradually downshifted while substrate permittivity is increased from 1 to 50. Therefore, the role of $LiNbO_3$ is evident. Simple single-loop split resonators (similar to SRR) and multiloop split (multisplit) resonators [2] have been compared. Among several tens of simulated structures with different numbers and mutual orientations of the individual resonators, we selected the one comprising two subwavelength single-loop resonators with gaps nearby and along the ground plane. The individual resonances were adjusted to obtain an operating regime, in which the inner resonator is moderately or weakly affected at its resonance

by the outer resonator, and vice versa, whereas the spectral distance between the resonances is no less than 30%.

In the proposed design, the side size of the inner split resonator is 2.4mm, the side size of the outer split resonator is 4mm, the gaps of the resonators are 0.2mm wide, and the wire radius is 0.62mm. The resonator-substrate block is placed at a distance of 0.2mm from the wire and 0.4mm from the ground plane, see Fig. 1. In the simulations, 18μm thick copper was used as the material for the subwavelength resonators. $LiNbO_3$ is an uniaxial anisotropic dielectric. At microwave frequencies, the nonzero components of its relative permittivity tensor are given by $\varepsilon_{xx} = \varepsilon_{yy} = 43$ and $\varepsilon_{zz} = 28$. Here, we only considered the case when the smaller value in the tensor corresponds to the direction along the wire, $z = w$, although two other cases. i.e., when it is either parallel to the ground plane, $z = u$, or perpendicular to the resonator plane, $z = v$, can also be used.

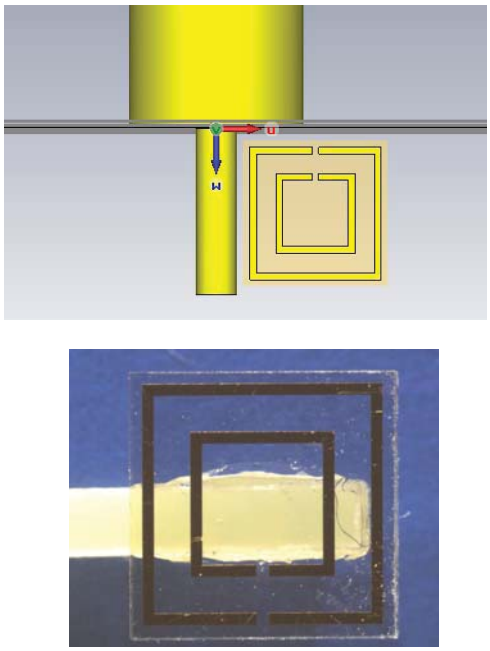

Fig. 1. Proposed antenna with two subwavelength resonators on $LiNbO_3$ substrate, which is fed by a coaxial transmission line (upper panel); photograph of the fabricated resonator-substrate block with holding bar (lower panel).

This choice of parameters allows us to obtain resonances at 2.8GHz and 4.2GHz, mainly due to the outer and the inner resonator, respectively, whereas the substrate itself does not work as a dielectric resonator antenna. Accordingly, for the first resonance, the resulting size of the antenna (i.e., all components located beyond the ground plane) is about $\lambda_0/18 \times \lambda_0/20 \times \lambda_0/80$, while the resonator-substrate block has a size of $\lambda_0/24 \times \lambda_0/24 \times \lambda_0/207$. For the second resonance, the sizes of the whole antenna and the resonator-substrate block are $\lambda_0/12 \times \lambda_0/14 \times \lambda_0/53$ and $\lambda_0/16 \times \lambda_0/16 \times \lambda_0/138$, respectively. Thus, the proposed antenna is ultra-miniature.

As follows from the obtained simulation results, the resonance frequencies can be slightly shifted by a fine adjustment of the location of the resonator-substrate block with respect to the wire. However, it may not be significantly shifted from the wire, since this can lead to a dramatic weakening of the coupling between the wire and the resonator-substrate block, worsening the output characteristics, and losing the ability of the proposed device to work as antenna at all. To fabricate antenna samples, *x*-cut $LiNbO_3$ wafers were patterned with 3μm thick gold using microfabrication techniques. Metal type and thickness were changed as compared to the simulations to better match the available fabrication techniques. The gap-bearing sides of the subwavelength resonators were aligned parallel to the *u*-axis. Finally, individual antennas were cut from the wafer using an automated dicing saw.

A low-ε bar was used to mechanically connect the resonator-substrate block with a positioner and fix it with respect to the wire. Being attached to the block at the back side, the bar weakly affects the resonance frequencies because of a high permittivity contrast between the materials of the bar and the substrate.

III. Results and Discussion

An HP8510C network analyzer was used to measure the S11. The results are presented in Fig. 2. Locations of the measured dips of S11 quite well coincide with the simulated ones. For the first band, the difference is less than 1%. For the second band, it is about 2%. This difference can be caused by inaccuracies in alignment of the resonator-substrate block and difference of the real material parameters and those used in simulations. The Q-factor measured at the -10dB level is equal to 47 and 68 for the first and the second resonance, while the corresponding simulated values are about 400. This difference can be connected, in particular, with the fact that the losses in $LiNbO_3$ were neglected in the simulations. The measured bandwidth is about 30MHz for the first band and 45MHz for the second band. The simulated radiation efficiency is about 10 percent for both bands, which is acceptable for such an ultra-miniature antenna, e.g., compare to [15,17].

The experiments were repeated for three different samples, which differ in the distance between the edge of substrate plate and the outer split resonator. The resonance frequencies and Q-factors have been found to be rather close for all three samples.

It has been shown by the simulations that the spectral location of the two resonance frequencies and, hence, the distance between them can be varied in a wide range by changing the location of the gaps while all other dimensions are fixed, or by changing the size of the resonators sides. This enables adjustment to the frequencies corresponding, for example, to WLAN, upper band Wi-Fi, 3G/4G cellular

networks, and WiMaX standards. The size of the resonator-substrate block can be further decreased.

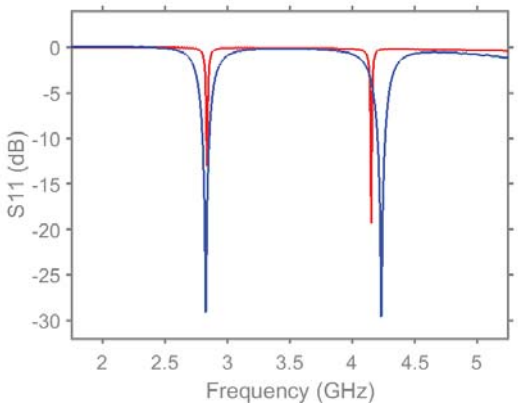

Fig. 2. S11-parameter: blue line - measurement, red line - simulation.

It has been shown by the simulations that the spectral location of the two resonance frequencies and, hence, the distance between them can be varied in a wide range by changing the location of the gaps while all other dimensions are fixed, or by changing the size of the resonators sides. This enables adjustment to the frequencies corresponding, for example, to WLAN, upper band Wi-Fi, 3G/4G cellular networks, and WiMaX standards. The size of the resonator-substrate block can be further decreased.

In a first set of preliminary radiation pattern measurements, the subwavelength-resonator based antenna was mounted in two different orientations corresponding to the variations of observation angle in the (u,w)- and (v,w)-planes. The receiving standard gain horn antenna was mounted at a distance of 100cm with two different orientations, in order to measure co- and cross-polarization. S21 was recorded for the four orientation combinations of the antenna and receiver. Figure 3 presents the measured radiation patterns. It is planned to perform a second set of radiation pattern measurements in the professional anechoic room of KU Leuven. The obtained data, including gain and efficiency, will be discussed during the presentation.

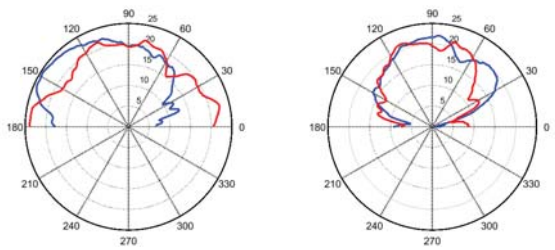

Fig. 3. Measured radiation patterns: left panel - (u,w)-plane, right panel - (v,w)-plane; blue lines - first resonance, red lines - second resonance.

IV. Conclusion

In this paper, we demonstrated by simulations and experiment how $LiNbO_3$ can be used for the miniaturization of a monopole antenna, i.e., beyond electrooptics, where this material is commonly used. The high extent of miniaturization is achieved due to the common effect of subwavelength resonators and the high permittivity of the $LiNbO_3$ substrate, which allows to decrease the resonance frequencies of the original (hypothetic) substrate-free structure by a factor of 2.8. The maximal dimension of the proposed ultra-miniature antenna in the first band is less than $\lambda_0/18$ and can further be decreased. The operating frequencies belong to S- and C-band. The results of the simulations show that they can be adjusted to various communication standards in the range from 1.5GHz to 6GHz, by modifying size and location of the split loops and size and location of the gaps in these loops. Future work may include experimental demonstration of other resonator-substrate combinations, with the aim to retrieve the basic features, extent, and limits of miniaturization, which occur while simultaneously using the effects of subwavelength resonators and high-permittivity substrate.

Acknowledgment

This work has been supported in part by the EU under the Marie Skłodowska-Curie Fellowship Program (project ADVANTA). A.E.S. thanks Dr. K.B. Alici and Dr. V. Volski for fruitful discussions.

References

[1] D. R. Smith, W. J. Padilla, D. C. Vier, S. C. Nemat-Nasser, and S. Schultz, "Composite medium with simultaneously negative permeability and permittivity," Phys. Rev. Lett. vol. 84, pp. 4184-4187, 2000.

[2] K. B. Alici, F. Bilotti, L. Vegni, and E. Ozbay, "Miniaturized negative permeability materials," Appl. Phys. Lett., vol. 91, 071121, 2007.

[3] W.-C. Chen, C.M. Bingham, K. M. Bingham, K. M. Mak, N. W. Caira, and W. J. Padilla, "Extreme subwavelength planar magnetic metamaterials," Phys. Rev. B, vol. 85, 201104, 2012.

[4] N. Engheta, A. Alu, R. W. Ziolkowski, and A. Erentok, "Fundamentals of waveguides and antenna applications involving double-negative (DNG) and single-negative (SNG) metamaterials," in Metamaterials: Physics and Engineering Explorations, N. Engheta and R. W. Ziolkowski, Eds., IEEE Press, 2006, pp. 43-85.

[5] H. R. Stuart and A. Pidwerbetsky, "Electrically small antenna elements using negative permittivity resonators," IEEE Trans. Ant. Propag., vol. AP-54, pp. 1644-1653, June 2006.

[6] K. B. Alici and E. Ozbay, "Electrically small split ring resonator antennas," J. Appl. Phys., vol. 101, 083104, 2007.

[7] I. W. Kwang and V. V. Varadan "Electrically small, millimeter wave dual band meta-resonator antennas," IEEE Trans. Ant. Propag., AP-58, pp. 3458-3463, Nov. 2010.

[8] P. Jin and R.W. Ziolkowski, "Metamaterial-inspired engineering of antennas," Proc. IEEE, vol. 99, pp. 1720-1731, Oct. 2011.

[9] P. Jin and R.W. Ziolkowski, "Multi-frequency, linear and circular polarized, metamaterial-inspired, near-field resonant parasitic

antennas," IEEE Trans. Ant. Propag., vol. AP-59, pp. 1446-1459, May 2011.

[10] C. G. M. Ryan and G. E. Eleftheriades, "Two compact, wideband, and decoupled meander-line antennas based on metamaterial concepts," IEEE Ant. Wireless Propag. Lett., vol. AWPL-11, pp. 1277-1280, 2012.

[11] S. Yan, P. J. Soh, and G. A. E. Vandenbosch, "Compact all-textile dual-band antenna loaded with metamaterial-inspired structure," IEEE Ant. Wireless Propag. Lett., vol. AWPL-14, pp. 1486-1489, 2015.

[12] S. Yan, X. Wang, Y. Hu, and G. A. E. Vandenbosch, "Low-profile omnidirectional antenna for automatic dependent surveillance – broadcast applications," Electron. Lett., vol. 51, pp. 1732-1734, 2015.

[13] E. Semouchkina, "Development of miniature microwave components by using high contrast dielectrics" in Microwave and Millimeter Wave Technologies from Photonic Bandgap Devices to Antenna Applications" in I. Minin, Ed., InTech, 2010, pp. 231-256. ISBN: 978-953-7619-66-4.

[14] A. E. Serebryannikov, M. Mutlu, and E. Ozbay, "Dielectric inspired scaling of polarization conversion subwavelength resonances in open ultrathin chiral structures," Appl. Phys. Lett., vol. 107, 221907, 2015.

[15] L. Lizzi, F. Ferrero, P. Mohin, C. Danchesi, and S. Boudaud, "Design of miniature antennas for IoT applications" in Proc. IEEE 6th International Conference on Communications and Electronics (ICCE), Ha Long, Vietnam, 2016; DOI: 10.1109/CCE.2016.7562642.

[16] M. Arif Khan, M. Aziz ul Haq, and S. ur Rehman, "A practical miniature antenna design for future internet of things enabled smart devices" in Proc. 10th International Conference on Signal Processing and Communication Systems (ICSPCS), Golden Coast, Australia, 2016; DOI: 10.1109/ICSPCS.2016.7843339.

[17] M. W. A. Khan, E. Moradi, L. Sydänheimo, T. Björninen, Y. Rahmat-Samii, and L. Ukkonen, "Miniature coplanar implantable antenna on thin andflexible platform for fully wireless intracranial pressure monitoring system," Int. J. Ant. Propag., 2017; DOI: 10.1155/2017/9161083.

[18] J.-W. Lian, Y.-L. Ban, Y.-L. Yang, L.-W. Zhang, C.-Y.-D. Sim, and K. Kang, "Hybrid multi-mode narrow-frame antenna for WWAN/LTE metal-rimmed smartphone applications," IEEE Access, vol. 4, 3991-3998, 2016.

[19] H. Chen and A. Zhao, "LTE antenna for mobile phone with metal frame," IEEE Ant. Wireless. Propag. Lett, vol. AWPL-15, pp. 1462-1465, 2016.

[20] W. S. T. Rowe and R. B. Waterhouse, "Efficient wideband printed antennas on lithium niobate," IEEE Trans. Ant. Propag., vol. AP-51, pp. 1413-1415, June 2003.

[21] Y. N. Wijayanto, A. Kanno, and T. Kawanishi, H. Murata and Y. Okamura, "Z-Cut $LiNbO_3$ optical modulator using patch antenna with orthogonal gaps for millimeter-wave radar applications" in Proc. 2014 Int. Topical Meeting on Microwave Photonics and the 2014 9th Asia-Pasific Microwave Photonics Conf., 20-23Oct. 2014, Sapporo, Japan.

[22] S. Wang and Q. Zhan, "Modified bow-tie antenna with strong broadband field enhancement for RF photonic applications" in Proc. SPIE, vol. 8806, 2013, pp. 88061V-1-88061V-6.

[23] T.-H. Lee, P.-I. Wu, and C.-T. Lee, "Integrated $LiNbO_3$ electrooptical electromagnetic field sensor," Microwave Opt. Technol. Lett., vol. 49, pp. 2312-2314, 2007.

[24] N. Kohmu, H. Murata, and Y. Okamura, "Electro-optic modulator using an antenna-coupled-electrode array and a polarization-reversed structure for a radar tracking system," Radio Sci. Bulletin, vol. 349, pp. 32-39, June 2014.